ADA-K ROUTING: BOOSTING THE EFFICIENCY OF MOE-BASED LLMS

Tongtian Yue[1,3], Longteng Guo[1,3], Jie Cheng[2,3], Xuange Gao[2,3], Jing Liu[1,3*]
[1]Zidongtaichu Foundation Model Research Center, CASIA
[2]State Key Laboratory of Multimodal Artificial Intelligence Systems, CASIA
[3]School of Artificial Intelligence, University of Chinese Academy of Sciences

ABSTRACT

In the era of Large Language Models (LLMs), Mixture-of-Experts (MoE) architectures offer a promising approach to managing computational costs while scaling up model parameters. Conventional MoE-based LLMs typically employ static `Top-K` routing, which activates a fixed and equal number of experts for each token regardless of their significance within the context. In this paper, we propose a novel `Ada-K` routing strategy that dynamically adjusts the number of activated experts for each token, thereby improving the balance between computational efficiency and model performance. Specifically, our strategy incorporates learnable and lightweight allocator modules that decide customized expert resource allocation tailored to the contextual needs for each token. These allocators are designed to be fully pluggable, making it broadly applicable across all mainstream MoE-based LLMs. We leverage the Proximal Policy Optimization (PPO) algorithm to facilitate an end-to-end learning process for this non-differentiable decision-making framework. Extensive evaluations on four popular baseline models demonstrate that our `Ada-K` routing method significantly outperforms conventional `Top-K` routing. Compared to `Top-K`, our method achieves over 25% reduction in FLOPs and more than 20% inference speedup while still improving performance across various benchmarks. Moreover, the training of `Ada-K` is highly efficient. Even for Mixtral-8x22B, a MoE-based LLM with more than 140B parameters, the training time is limited to 8 hours. Detailed analysis shows that harder tasks, middle layers, and content words tend to activate more experts, providing valuable insights for future adaptive MoE system designs. Both the training code and model checkpoints will be publicly available.

1 INTRODUCTION

Over the past few years, the rapid development of Large Language Models (LLMs) (Brown et al., 2020b; Raffel et al., 2020; Touvron et al., 2023a; Chiang et al., 2023) has marked a significant leap towards Artificial General Intelligence (AGI). Generally, increasing the number of parameters in an LLM enhances its performance across diverse tasks, demonstrating emergent capabilities (Kaplan et al., 2020; Brown et al., 2020a). However, this improvement comes with substantial computational costs for both training and inference, posing barriers to the broad application and efficiency.

In response to these challenges, the Mixture-of-Experts (MoE) (Jacobs et al., 1991; Eigen et al., 2013) architecture has gained popularity as a scalable solution that balances parameter increase with computational cost. MoE implementations in Transformers (Vaswani et al., 2017) have shown that significant model scaling can be achieved without a proportional rise in computational burden, thus maintaining efficient performance. These successes highlight the promising potential of MoE-based LLMs (Jiang et al., 2024; Team; Dai et al., 2024).

The core of the MoE architecture comprises a set of expert networks governed by a routing strategy. This routing strategy, executed via a learnable router (Fedus et al., 2022a; Du et al., 2022a), selectively assigns each token to a limited number of experts. This sparse expert selection is pivotal for MoE efficiency. The most common routing strategy is `Top-K` routing (Shazeer et al., 2017b). It selects the best-suited experts for each input based on preliminary probability calculations, activating the top k

*Corresponding author.

experts. Although recent studies (Zoph et al., 2022; Lewis et al., 2021a) have introduced adjustments to ensure more balanced activation across experts, a major limitation remains: the fixed activation numbers does not account for the varying importances of different tokens.

The importances of tokens can vary significantly, potentially influenced by factors such as the different demands of tasks (Rogers et al., 2021), the inherent characteristics of words (Schick & Schütze, 2020), and the contexts in which they are used (Guu et al., 2020). This oversight of token differences can lead to resource inefficiencies. Simpler tokens with minimal semantic significance may receive more processing power than needed, leading to inefficiencies. Conversely, more complex tokens—those representing critical information or requiring advanced logical reasoning—might not get adequate attention. This misallocation of expert resources not only suboptimizes performance but also hinders further improvements in computation efficiency.

To address the limitations of traditional `Top-K` routing in MoE models, we propose a novel, learnable `Ada-K` routing strategy that adapts expert allocation based on each token's inherent importance and difficulty. Specifically, this strategy introduces a pluggable, lightweight allocator, easily integrable into existing MoE-based LLMs. The allocator dynamically determines the optimal number of experts for each token by sampling from the probability distribution it outputs over the possible expert counts. However, this sample operation is inherently non-differentiable. Hence, we employ the Proximal Policy Optimization (PPO) algorithm (Stiennon et al., 2020; Nakano et al., 2021) to optimize the allocators end-to-end, towards ideal balance between model performance and efficiency.

We validate the effectiveness of our proposed `Ada-K` routing strategy by integrating it into four popular MoE-based LLMs and assessing their performance across multiple benchmarks. Compared to baseline models utilizing `Top-K` routing, our `Ada-K` routing consistently reduces the number of activated experts by 30% to 40%, while simultaneously enhancing overall performance. This reduction in expert activation directly translates to computational gains, achieving more than a 25% reduction in FLOPs and a 20% speedup in inference time. Notably, this favorable balance is attained with minimal additional training, requiring the tuning of only approximately 2M parameters, with training times under 8 hours for all baseline models.

Furthermore, we conduct a detailed analysis of the `Ada-K` routing strategy at the task, layer, and token levels. Our findings indicate that harder tasks, middle layers, and content words tend to activate more experts, demonstrating the strategy's ability to allocate computational resources efficiently based on the importance of input tokens. These conclusions also provide valuable insights for future adaptive MoE system designs. Our contributions are summarized as follows:

- **An advanced dynamic routing strategy.** We propose a dynamic `Ada-K` routing strategy that adjusts the activated experts number on a per-token basis to enhance the conventional `Top-K` routing. Compared to `Top-K` routing, `Ada-K` routing manages to save over 25% FLOPs and achieve more than 20% acceleration in inference, while enhancing performance.
- **An efficient RL-based training framework.** We introduce a learnable and lightweight allocator module that determines the optimal number of activated experts for each token through end-to-end training. Reinforcement learning techniques have been carefully designed and introduced to facilitate the training of this non-differentiable decision-making framework.
- **Comprehensive quantitative and qualitative experiments.** We extensively evaluate our method across four popular MoE-based LLMs, ranging from 14.3B to 140B parameters. `Ada-K` routing demonstrates consistent advantages over these baselines. The effectiveness of our proposed method is further validated by extensive qualitative analyses.

2 Related Work

2.1 Mixture-of-Experts

The sparse Mixture-of-Experts (MoE) layer, which includes a predetermined number of experts and a routing network, is initially introduced to enhance the capacity of deep neural networks for NLP tasks in LSTM models (Shazeer et al., 2017a). This architecture is later extended to Transformers (Lepikhin et al., 2020) and adapted for computer vision (Riquelme et al., 2021; Daxberger et al., 2023), gaining popularity due to its robust scaling properties (Du et al., 2022b; Clark et al., 2022). In the MoE framework, extensive research has focused on refining routing algorithms (Hazimeh et al., 2021; Lewis et al., 2021b; Roller et al., 2021; Zhou et al., 2022). Approaches range from random

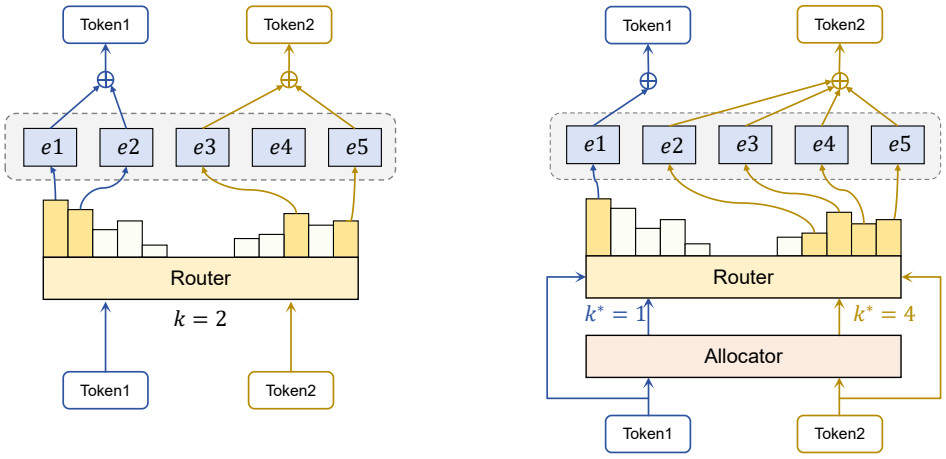

(a) Top-K Routing MoE (b) Ada-K Routing MoE

Figure 1: Comparison of `Top-K` and `Ada-K` routing strategies for MoE: (a) In `Top-K` routing, each token consistently selects a fixed number of k experts based on predefined model configuration. (b) In `Ada-K` routing, each token dynamically activates a customized number of experts via our newly introduced learnable allocator module.

routing (Zuo et al., 2021) and activating all experts via weighted averages (Eigen et al., 2013), to selectively engaging a single or multiple experts (Fedus et al., 2022b; Du et al., 2022b). However, they universally deploy a fixed number of experts, irrespective of the differing complexities of input tokens (Lepikhin et al., 2020; Fedus et al., 2022b). In our study, we introduce a parameter-efficient and data-efficient training framework that introduces lightweight learnable modules, *i.e.* allocators. These allocators seamlessly work with routers to dynamically assign expert resources across individual tokens. Our framework markedly reduces computational costs while achieving improved performance compared to the baseline models.

2.2 Reinforcement Learning in LLMs

Recent advancements in Large Language Models (LLMs) have been significantly influenced by Reinforcement Learning (RL). For instance, the Reinforcement Learning from Human Feedback (RLHF) approach has demonstrated efficacy in aligning LLMs with human-centric values and preferences (Bai et al., 2022; Ouyang et al., 2022; Cheng et al., 2024). This method involves training a reward model (RM) that encapsulates human preferences and subsequently refining LLMs based on the reward signals generated by the RM. Additionally, some studies (Lee et al., 2023; Xu et al., 2023; Yue et al., 2024) have investigated the LLM-centric multimodal representation learning, utilizing RL to improve the alignment between the semantic spaces of LLMs and visual concepts. Typically, they often leverage the Proximal Policy Optimization (PPO) algorithm (Stiennon et al., 2020; Nakano et al., 2021) to perform parameter optimization. In this work, we present a novel PPO-based training framework tailored for MoE, a widely-used architecture in modern LLMs. This plug-and-play framework seamlessly integrates with MoE models and its variants. We execute end-to-end agents training via RL, with these agents tasked with resource scheduling for expert activation, thereby significantly enhancing the inference efficiency.

3 Method

3.1 Top-K Routing

We begin by providing a concise overview of the sparse `Top-K` routing MoE model. Structurally, an MoE layer substitutes the feed-forward network (FFN) sub-block of the original Transformer layer with an expert network comprising N experts $E = \{e_1, e_2, ..., e_N\}$. For each token x_i in the input sequence X, the activation probabilities for each expert are determined via a router layer W:

$$\mathcal{P}(x_i) = \text{Softmax}\left(W \cdot x_i\right) \tag{1}$$

with $W \in \mathbb{R}^{C \times N}$ being a lightweight, trainable projection matrix. `Top-K` routing MoE employs a routing strategy where the k experts with the highest weights in $\mathcal{P}(x_i)$ are selected. The weights of

the chosen experts are then normalized, while that of the remaining experts are set to zero, indicating their inactivity:

$$g(x_i) = \frac{\mathcal{P}(x_i)}{\sum_{j \in TopK(\mathbf{P})} P_j} \cdot \mathbf{1}_{i \in TopK(\mathbf{P})} \tag{2}$$

where $\mathbf{1}_{i \in TopK(\mathbf{P})}$ is an indicator function that is 1 if $i \in TopK(\mathbf{P})$ and 0 otherwise. The final output, derived from $g(x_i)$, is a weighted average of the k chosen experts:

$$\text{MoE}(x_i) = \sum_{n=1}^{N} g_n(x_i) \cdot e_n(x_i) \tag{3}$$

3.2 ADA-K ROUTING

In this section, we introduce the proposed `Ada-K` routing framework outlined in Figure 1. It enhances the conventional `Top-K` routing by incorporating a novel component called allocator. The allocator works synergistically with the original router to dynamically perform expert allocation for each token x_i. Structurally, the allocator is a lightweight, trainable linear layer, similar to the router, and is responsible for determining the optimal number of experts k^* for each token. The allocator takes x_i as the input and then produces a probability distribution over the possible number of experts, from which k^* is obtained through probability-based sampling. Subsequently, k^* and x_i are passed to the router, which then activates the top k^* experts to produce the weighted representations as described in Sec 3.1.

3.3 LEARNING STRATEGY

In our proposed framework, the entire training strategy is specifically tailored to the newly introduced allocators, with the original LLM maintained in a frozen state to preserve its inherent capabilities. The training objective is to enhance both performance and efficiency, which can be decomposed into optimizing linguistic capabilities and minimizing the average number of activated experts. Regarding linguistic capabilities, direct optimization via backpropagation is precluded due to the non-differentiable nature of sampling from distributions during the forward pass. To address this challenge, we leverage reinforcement learning (RL), which circumvents the need for differentiable action sampling. Regarding the activated expert counts, we incorporate a regularization loss to minimize the expectation value of the allocator's output distribution.

PPO Loss. In the setting of RL, the allocator of l-th layer is considered as an *agent* with a policy π parameterized by θ_l. We introduce a warm-start strategy to initialize θ_l, which will be discussed later.

The representation of x_i at l-th layer is regarded as the *state* s_l. The number of activated experts $\hat{c}_l$, determined through sampling, serves as the *action* taken under policy π_{θ_l}, *i.e.*, $\hat{c}_l \sim \pi_{\theta_l}(\cdot|s_l)$. The objective is to maximize the expected return $\mathbb{E}[\sum_{l=1}^{L} \gamma^{l-1} R(\hat{c}_l, s_l)]$ over the policy π, where γ serves as the discounted factor, $\gamma \in (0, 1]$, and L represents the number of layers in the model. We define the reward as follows:

$$R(\hat{c}_l, s_l) = \log \mathcal{P}(x_i|x_1, \ldots, x_{i-1}) \cdot \mathbf{1}_{l=L} \tag{4}$$

where only the allocator at the last layer receives the log likelihood as the reward. In other words, Eq. (4) could be simplified as $\mathbb{E}[\gamma^{L-1} \log \mathcal{P}(x_i|x_1, \ldots, x_{i-1})]$. Through the reward defined in this way, maximizing the expected return is equivalent to minimizing caption loss in NLP. We employ the PPO algorithm (Stiennon et al., 2020; Nakano et al., 2021) to optimize the policy within the trust region for stable training. The RL loss function is formulated as follows:

$$\mathcal{L}^{RL}(\theta) = -\mathbb{E}_l \left[\min\left(r(\theta_l)A_l,\ \text{clip}\left(r(\theta_l), 1-\epsilon, 1+\epsilon\right) A_l\right)\right] \tag{5}$$

where ϵ is a hyperparameter and clip function is introduced to constrain values within a specified range. The importance sampling ratio $r(\theta_l)$ is formulated as follows:

$$r(\theta_l) = \frac{\pi_{\theta_l}(\hat{c}_l|s_l)}{\pi_{\theta_l^{\text{old}}}(\hat{c}_l|s_l)} \tag{6}$$

where θ_l^{old} is the policy parameters before update.

In standard PPO algorithm, it needs another value function to compute the advantage, which requires additional network and computations. Alternatively, we apply the form of advantage function in *reinforce with baseline* algorithm (Sutton & Barto, 2018) formulated in Eq.(7), where the baseline is employed to reduce variance theoretically:

$$A_l(\hat{c}_l, s_l) = \sum_{m=l}^{L} \gamma^{m-l} \left[R(\hat{c}_m, s_m) - R(c_m^*, s_m^*) \right] = \gamma^{L-l} \left[R(\hat{c}_L, s_L) - R(c_L^*, s_L^*) \right] \tag{7}$$

The superscript * denotes the baseline, which is define as default `Top-K` routing. There is no need of gradients for action $\hat{c}_l$, reward $R(\hat{c}_l, s_l)$, advantage $A(\hat{c}_l, s_l)$, and old sampling probability $\pi_{\theta_l^{\text{old}}}(\hat{c}_l|s_l)$, only latest sampling probability $\pi_{\theta_l}(\hat{c}_l|s_l)$ needs to calculate gradient in training loss.

Activation Regularization Loss. The regularization loss reduces the activated expert counts by optimizing the expectation of the distribution produced by every allocator:

$$\mathcal{L}^{reg}(\theta) = \frac{1}{L} \sum_{l=1}^{L} \sum_{n=1}^{N} i \cdot \mathcal{P}_{\theta_l}(i) \tag{8}$$

The final loss is a combination of the PPO loss and regularization loss, where λ is a hyper-parameter to control the reduction degree of the activated expert counts.

$$\mathcal{L}(\theta) = \mathcal{L}^{RL}(\theta) + \lambda \mathcal{L}^{reg}(\theta) \tag{9}$$

Warm Start. Given the large decision space encompassing all expert counts, allocators require an effective parameter initialization to mitigate instability and inefficiency caused by arbitrary or incorrect choices. In this paper, we propose a warm-start approach "***P-Warm***" to pre-train the allocators. This pre-training process utilizes the nucleus sampling (Holtzman et al., 2019) (*i.e.*, Top-P) to generate pseudo-labels. Specifically, we first choose the minimal subset of experts whose cumulative probability, as determined by the original router, surpasses the threshold p. As illustrated in the Eq.(10), for a given token x_i, the number of experts within the subset is denoted by $n_i(p)$:

$$n_i(p) = \underset{k \in \{1 \ldots, N\}}{argmin} \sum_{j<=k} \mathcal{P}_{i,j}^{\downarrow} \geq p \tag{10}$$

where $\mathcal{P}_{i,j}^{\downarrow}$ represents the probability distribution arranged in descending order. For each MoE baseline model, we compute the average expert counts across different p values using a moderate amount of token set T. The p value whose average counts is closest to the default activation value, *i.e.* k, is then selected.

$$p^* = \underset{p}{argmin} \, |\frac{1}{T} \sum_{i=1}^{T} n_i(p) - k|. \tag{11}$$

Finally, for every token x_j in the training dataset, we utilize $n_j(p^*)$ as pseudo labels to facilitate the warm start training of the allocators.

4 Experiments

4.1 Implementation Details

Model Settings. We verify the effectiveness and universality of our proposed training framework on four prevailing MoE based LLMs, *i.e.* Mixtral-8x22B (Jiang et al., 2024), Mixtral-8x7B (Jiang et al., 2024), DeepSeek-MoE-16B (Dai et al., 2024) and Qwen1.5-MoE-A2.7B (Team). The architectural details of the four baseline models are presented in Table 1. Mixtral-8x7B and Mixtral-8x22B utilize a standard `Top-K` routing strategy for all experts. Additionally, DeepSeek-MoE-16B and Qwen1.5-MoE-A2.7B classify experts into shared and routed categories. Each token inherently activates all shared experts and selects the `Top-K` experts from the routed categories. `Ada-K` is applicable to any routing-based expert module. Besides, we keep the shared experts when present.

Table 1: Architecture details of four baseline models.

Config	Mixtral 8x22B	Mixtral 8x7B	DeepSeek MoE-16B	Qwen1.5 MoE-A2.7B
Top-K	2	2	6	4
Shared Experts	0	0	2	4
Routed Experts	8	8	64	60
MoE Layers	56	32	27	24
Activated Params	39.0B	12.9B	2.8B	2.7B
Total Params	140.6B	46.7B	16.4B	14.3B

Benchmark and Evaluation Details. Following previous works (Touvron et al., 2023b; Le Scao et al., 2023; Li et al., 2023; Black et al., 2022), we employ the lm-evaluation-harness (Gao et al., 2021) to evaluate our model. This tool serves as the backend for the HuggingFace Open LLM Leaderboard (Beeching et al., 2023). Our model is assessed on 6 key benchmarks aligned with Open LLM Leaderboard, *i.e.*, AI2 Reasoning Challenge (ARC-C) (Clark et al., 2018), HellaSwag (Hella) (Zellers et al., 2019), MMLU (Hendrycks et al., 2020), TruthfulQA (Truth) (Lin et al., 2021), Winogrande (Wino) (Sakaguchi et al., 2021) and GSM8K (GSM) (Cobbe et al., 2021). Refer to Appendix for additional details about benchmarks.

For the evaluations, we assess performance across two dimensions. First, we examine the model's accuracy across various benchmarks. Second, we evaluate the computational cost of the model with `Ada-K` routing. Specifically, we utilize four metrics: average activated expert counts per token (Act), activation reduction rate (Rate), total floating point operations (FLOPs), and inference time speedup (Speedup). "Rate" is calculated as $(1 - Act/k) \times 100\%$, where k represents the default activation value. "Speedup" is the cumulative total across six benchmarks and "FLOPs" is measured by one single sample with a length of 256.

Training Details. We adopt AdamW (Loshchilov & Hutter, 2017) as the optimizer. All baseline models are trained for one epoch using a consistent set of 10k samples. The batch size and learning rate is set to 64 and 1e-3, respectively. We leverage 2 PPO epochs for reinforcement learning. For all four baseline models, we uniformly set λ as 3e-3. This ratio prioritizes ensuring a sufficient reduction rate, while guarantee a performance advantage over the original model. The training overhead for `Ada-K` is relatively efficient. As shown in Table 2, the trainable parameters for all baseline models are on the scale of 1M, which is negligible compared to the total parameters. Additionally, we present the training hours for the four baseline models. We employ 16 NVIDIA A800 GPUs to train Mixtral 8x22B, whereas each of the other three utilizes 8 NVIDIA A800 GPUs. The training time for all baseline models is limited to 8 hours. Further details can be found in the Appendix.

Table 2: Training overhead of four baseline models.

Baseline Model	Total Params	Trainable Params	Training Hours
Mixtral-8x22B	140.6B	2.75M	7.92h
Mixtral-8x7B	46.7B	1.05M	4.96h
DeepSeek-MoE-16B	16.4B	3.54M	1.79h
Qwen1.5-MoE-A2.7B	14.3B	2.95M	1.58h

4.2 Performance Evaluation

Table 3: Performance for four baseline models across six benchmarks. Results using default `Top-K` routing and our method are highlighted in brown and blue, respectively. Each arrow and its associated numeric annotation indicate the performance disparity with the default `Top-K` baseline.

Method	Accuracy							Computation			
	ARC-C	Hella	MMLU	GSM	Truth	Wino	Average	Act ↓	Rate ↑	FLOPs ↓	Speedup ↑
Mixtral-8x22B											
`Top-K` ($k=1$)	66.22	85.43	73.15	70.96	61.54	82.77	73.35 ↓5.80	1.00	50.0%	11.38T	1.39×
`Top-K` ($k=2$)	72.70	89.08	77.77	82.03	68.14	85.16	79.15	2.00	0.0%	20.04T	1.00×
`Ada-K`	73.57	89.76	78.22	82.98	69.97	85.02	79.92 ↑0.77	1.31	34.4%	14.08T	1.31×
Mixtral-8x7B											
`Top-K` ($k=1$)	60.41	83.13	64.71	40.71	34.67	75.77	59.90 ↓7.68	1.00	50.0%	3.68T	1.35×
`Top-K` ($k=2$)	66.72	86.48	70.39	58.38	41.25	82.24	67.58	2.00	0.0%	6.56T	1.00×
`Ada-K`	68.49	87.23	70.40	58.61	42.85	81.45	68.19 ↑0.61	1.40	30.0%	4.42T	1.28×
Qwen1.5-MoE-A2.7B											
`Top-K` ($k=2$)	51.88	77.99	59.20	14.21	38.87	70.11	52.04 ↓2.39	2.00	50.0 %	0.88T	1.25×
`Top-K` ($k=3$)	52.78	78.69	60.65	14.78	40.96	72.20	53.34 ↓1.09	3.00	25.0 %	1.00T	1.14×
`Top-K` ($k=4$)	54.69	79.45	61.30	15.62	42.50	73.00	54.43	4.00	0.0%	1.23T	1.00×
`Ada-K`	54.41	79.65	60.99	21.21	41.96	72.53	55.13 ↑0.70	2.58	35.5%	0.92T	1.22×
DeepSeek-MoE-16B											
`Top-K` ($k=3$)	51.37	78.33	40.11	12.59	30.16	72.22	47.46 ↓2.45	3.00	50.0%	0.96T	1.27×
`Top-K` ($k=4$)	52.73	79.44	43.04	14.86	30.34	72.88	48.87 ↓1.04	4.00	33.3%	1.08T	1.18×
`Top-K` ($k=5$)	52.39	79.71	44.00	15.30	30.92	73.72	49.34 ↓0.57	5.00	16.7%	1.20T	1.08×
`Top-K` ($k=6$)	52.22	79.84	44.72	16.45	31.07	75.14	49.91	6.00	0.0%	1.36T	1.00×
`Ada-K`	53.44	80.24	44.98	16.86	31.83	75.92	50.55 ↑0.64	3.61	40.0%	1.00T	1.24 ×

For the four baselines, the relevant accuracy and computation metrics (detailed in Sec 4.1) are reported in Table 3. Additionally, we present the metrics of the baseline models under a lower `Top-K`

activation level (*e.g.*, $k = 1$ for Mixtral-8x7B) as a supplementary comparison. The implementation of Ada-K routing leads to a significant and consistent improvement in accuracy across all baselines compared to the default settings. This enhancement is particularly noteworthy, as models employing Ada-K routing not only achieve these accuracy gains but also reduce FLOPs by over 25% and accelerate inference by more than 20%, demonstrating a compelling balance between performance and efficiency. We believe these results arises from a more effective expert resource allocation.

4.3 Ablation Study

In this section, we perform a comprehensive ablation analysis of the proposed training framework. It should be noted that the conclusions are consistent across four baseline models. However, due to space limitations, we uniformly present the numerical results based on Qwen1.5-MoE-A2.7B.

Trade-off between performance and activation reduction rate. We first investigate the trade-off between the activation reduction rate and model performance. As detailed in Sec 4.1, the results in Table 3 are based on a fixed value of λ (*i.e.*, 3e-3) in Equation 9. Actually, Ada-K could facilitates a more flexible balance between accuracy and computational efficiency through it. By varying λ, we generate 15 data points to construct the trade-off curve illustrated in Figure 2. The trade-off point in the figure correspond to Table 3. Analysis reveals that, prior to the trade-off point, accuracy declines gradually with increasing activation reduction. However, beyond this point, the rate of decline accelerates sharply. Importantly, our method consistently surpasses the default Top-K model until the activation reduction rate reaches approximately 44%. Compared to traditional Top-K routing, Ada-K provides both adjustable flexibility and a more effective balance between performance and efficiency.

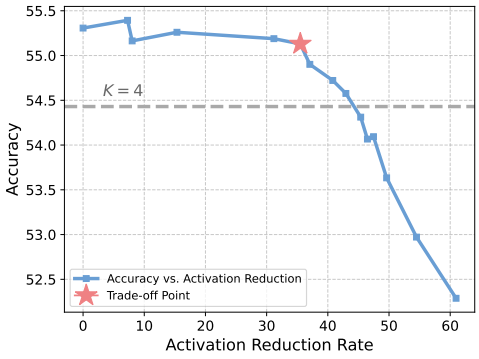

Figure 2: Trade-off curve between performance and activation reduction rate.

Effect of dynamic routing. To the best of our knowledge, Ada-K is the first learnable dynamic expert allocation strategy. In this section, we aim to explore and validate the advantages of this pure dynamic paradigm. Actually, as shown in Table 3, at comparable activation reduction rates, baseline models with lower Top-K activation levels exhibit a significant performance gap when compared to Ada-K routing. To adapt these baseline models, which have reduced numbers of active experts, to their new activation patterns, we fine-tune their routers using the same 10K dataset as Ada-K. This process effectively imparts a pseudo-dynamic quality to the static Top-K routing. Additionally, some prior works (*e.g.*, MoE-D (Huang et al., 2024) and D2DMoE (Piórczyński et al., 2023) achieve quasi-dynamic routing through fixed thresholds. They determine the activation of each expert by comparing the routers' output against these thresholds. We also include these methods in our comparison by reproducing them using their official code. The results in Table 4 suggest that improving the adaptability of static routing leads to modest performance gains relative to the original baselines. Additionally, threshold-based routing demonstrates a slight advantage over static routing. However, these methods still fall significantly short compared to Ada-K, highlighting the critical need for a dynamic and efficient expert allocation strategy.

Table 4: Ablation study about the dynamic routing. The results of default Top-K routing and our method are highlighted in brown and blue, respectively.

Route	Tuned	Acc	Rate
Top-K ($k = 2$)	✗	52.54 ↓1.89	50.0%
	✓	52.85 ↓1.58	50.0%
Top-K ($k = 3$)	✗	53.34 ↓1.09	25.0%
	✓	53.44 ↓0.99	25.0%
Top-K ($k = 4$)	✗	54.43	0.0%
	✓	53.89 ↓0.54	0.0%
MoED ($p = 0.3$)	✓	53.45 ↓0.98	32.4%
MoED ($p = 0.4$)	✓	53.60 ↓0.83	28.6%
D2D ($\tau = 0.1$)	✓	53.73 ↓0.70	27.8%
D2D ($\tau = 0.2$)	✓	53.64 ↓0.79	31.5%
Ada-K	✓	55.13 ↑0.70	35.5%

Effect of activation regularization. In this section, we explore different schemes for reducing expert activations. The related results are reported in Table 5. Since the expectation of each allocator's output distribution is differentiable, it allows for direct optimization via backpropagation (row "As Loss"). So we choose it as the default method. Alternatively, combining the language modeling likelihood and the activate expert count of each token to form a reward presents another viable strategy (row "As Reward"). It introduces a reward-level trade-off where all training objectives are uniformly optimized through the PPO loss. For fair comparison, we employ the same training data and ensure consistent activation reduction rates. The results indicate that direct optimization of expectations yields marginally better performance than treating them as rewards. However, the difference is not significant. It highlights the effectiveness and robustness of `Ada-K` routing training.

Table 5: Ablation study about the activation regularization methods. The results of default `Top-K` routing and our method are highlighted in brown and blue, respectively.

Method	Acc	Act	Rate
Original	54.43	4.00	0.0%
As Reward	54.64 ↑0.21	2.56	36.0%
As Loss	55.13 ↑0.70	2.58	35.5%

Effect of training data. In this section, we examine the impacts of varying training data, *i.e.* pretrain and supervised fine-tuning (SFT) data. For fairness, each data type comprises 10k samples sourced from prominent open-source corpus. We report the training results in Table 6. The results indicate that the training is not sensitive to the data domain. It achieves comparable performance across two data settings, demonstrating both the effectiveness and robustness of `Ada-K` routing training. We detail the collection and organization processes for two types of data in the Appendix.

Table 6: Ablation study about the training data type. The results of default `Top-K` routing and our method are highlighted in brown and blue, respectively.

Data Type	Acc	Act	Rate
Original	54.43	4.00	0.0%
Pretrain	55.78 ↑1.35	2.68	33.0%
SFT	55.13 ↑0.70	2.58	35.5%

Effect of warm up strategy. In this section, we conduct an ablation study on different warm start strategies. The results are reported in Table 7. If no warm-up strategy is employed, the allocators are initialized randomly (the second row). The *K-Warm* strategy involves pretraining the allocators to consistently output k. For *P-Warm*, as detailed in Sec 3.3, pseudo-labels are generated using a specific p value. The findings indicate that both the *K-Warm* and *P-Warm* strategies obviously surpass the performance of the default baseline, whereas the random strategy shows only comparable performance. It is largely due to the pre-training mitigates the sampling arbitrariness caused by random initialization, facilitating the learning of more optimal strategies. Additionally, the more flexible warmup strategy *P-Warm* yields marginally improved performances compared to the static *K-Warm*.

Table 7: Ablation study about the warm up strategy. The results of default `Top-K` routing and our method are highlighted in brown and blue.

Strategy	Acc	Act	Rate
Original	54.43	4.00	0.0%
✗	54.18 ↓0.25	2.88	28.0%
K-Warm	54.97 ↑0.54	2.60	35.0%
P-Warm	55.13 ↑0.70	2.58	35.5%

4.4 Visualization and Analysis

In this section, we provide a detailed analysis and visualization of the policies learned by the agents (*i.e.*, allocators) after training with `Ada-K` routing. Due to space limitations, we uniformly present the numerical results based on Qwen1.5-MoE-A2.7B.

Expert resource allocation is more adaptive. We initially analyze the probability distribution of activated expert counts per token: $\mathcal{P}(k) = \frac{r(k)}{\sum_{n=1}^{N} r(n)}$, where $r(k)$ represents the number of tokens activating k experts. The results for each benchmark are illustrated in Figure 3 using a logarithmic scale for enhanced clarity. The analysis reveals: (1) The decision space available to trained allocators ranges from 1 to the total number of experts, ensuring adaptive resource allocation. (2) The training effectively reduces the activation levels of the majority of tokens to approximately 2 or 3. Concurrently, around 10% of essential tokens are identified and subjected to enhanced processing by engaging more than the default number of experts. (3) The expert activation distribution differs

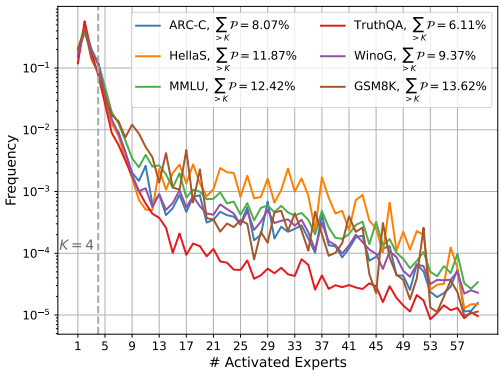

Figure 3: Probability distribution curves of expert activations per token across six benchmarks.

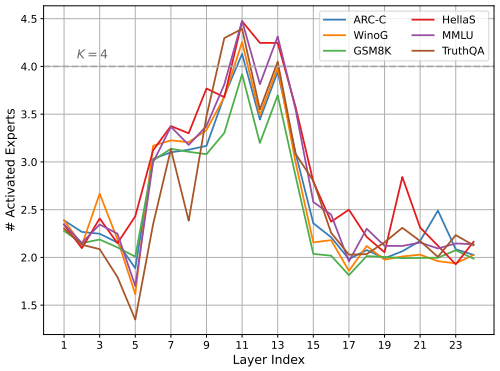

Figure 4: Curves of expert activations per layer across six benchmarks.

across benchmarks, demonstrating that the trained allocators are capable of adapting to diverse domains and devise customized solutions accordingly.

Middle layers tend to activate more experts. As illustrated in Figure 4, variations in layer depth consistently impact average expert activations across multiple benchmarks. Specifically, both the shallow and deep layers utilize fewer experts, whereas the intermediate layers employ a higher number of experts. We hypothesize that this can be attributed to the varying complexities at different stages of processing. Shallow layers mainly engage in basic feature extraction, *e.g.* recognizing simple syntactic patterns and semantic elements, which might generally necessitates minimal specialized knowledge and thus reduces the requirement for experts. Conversely, middle layers might play a pivotal role in more intricate tasks, including the integration of basic features into sophisticated representations, ambiguity resolution, and the comprehension of contextual nuances. These tasks could likely benefit from a diverse array of specialized inputs, possibly necessitating a larger pool of experts to enhance the processing robustness. In contrast, deep layers might primarily concentrate on refining these integrated features and finalizing the output, mainly involving the application and optimizing of processed information, which can typically be achieved with fewer experts.

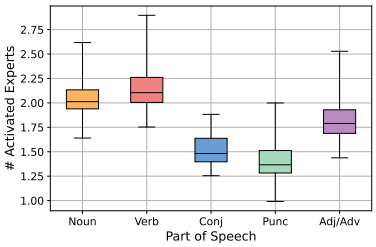

Figure 5: Average expert activation number per token across different parts of speech.

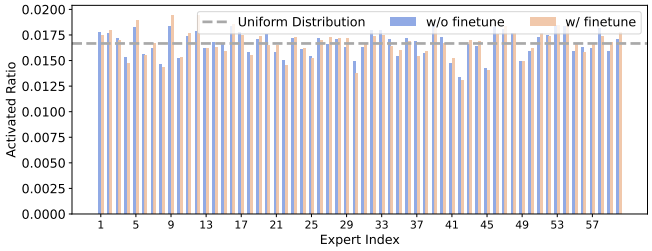

Figure 6: Distribution curves of expert workloads before and after `Ada-K` fine-tuning. The gray horizontal line represents the uniform distribution of expert activations.

Content words tend to activate more experts. To evaluate the impact of token attributes, we statistically analyze both part-of-speech (POS) and expert activations for a total of 51 million tokens across six benchmarks. To reduce variability due to randomness, our analysis only includes tokens that occur more than 1,000 times within these corpora. POS tagging is performed using the NLTK toolkit (Bird, 2006). We calculate average activations for prevalent POS categories, namely nouns, verbs, conjunctions, adjectives/adverbs, and punctuation. The findings presented in Figure 5 suggest that enhanced expert resource tends to concentrate on verbs and nouns, which are central to syntactic construction and convey clear semantic meanings. In contrast, the expert activations on elements with weaker semantic content, *e.g.* special symbols and conjunctions, are relatively less. This conclusion largely substantiates the intuitive basis for our research motivation. The strategies learned by the agents (*i.e.*, allocators) tend to allocate more expert resources to tokens rich in semantic information, allowing for thorough modeling. Conversely, tokens with weaker semantics require only minimal

expert resources for effective representation. This more rational resource allocation strategy benefits both semantic understanding and computational efficiency.

Load balance is maintained. In this section, we investigate whether the previously established expert load balance of the default `Top-K` model is maintained after fine-tuning with our `Ada-K` routing. Intuitively, since the router that determines expert allocation remains frozen throughout the training process, our framework is anticipated to minimally disturb the original load balance. We assess the activation probability of each expert across six benchmarks, as illustrated in Figure 6. The results demonstrate that the load on each expert remains nearly unchanged before and after training, preserving a nearly uniform distribution.

Table 8: Average activated experts and accuracy delta across tasks of varying difficulty levels. ΔAcc represents the absolute performance improvement compared to default `Top-K` routing.

Benchmarks	Act	ΔAcc
ARC-E	2.23	-0.40
ARC-C	2.84	+0.12
Collection	2.58	+0.70
BBH	3.43	+5.54

Table 9: The relationship between the ratio of layers equipped with the allocator to all layers and the corresponding metrics. The results with default setting are highlighted in blue.

Ratio	Training Params	Training Time	Acc	FLOPs
0.125	0.37M	1.54h	54.98	1.19T
0.25	0.74M	1.55h	55.06	1.14T
0.5	1.48M	1.56h	55.15	1.04T
1.00	2.95M	1.58h	55.13	0.92T

Hard tasks tend to activate more experts. As shown in Table 8, we examine the effect of task difficulty on activated expert counts across both intra-benchmark and inter-benchmark dimensions. For both dimensions, we report the average number of activated experts and the performance gains (relative to the default `Top-K` setting) of our method. For intra-benchmark dimension, we leverage ARC, a multiple-choice question-answering dataset consisting of science exam questions for grades 3 to 9, we analyze two levels of task difficulty, namely Easy (E) and Challenge (C). For inter-benchmark dimension, we compare the commonly used six benchmarks (detailed in Sec 4.1) with BBH (BIG-Bench Hard) (Suzgun et al., 2022). BBH comprises 23 demanding tasks that require sophisticated cognitive skills such as multi-hop reasoning, causal inference, and logical deduction, markedly exceeding the difficulty of the collection of six benchmarks. The results indicate that model with `Ada-K` routing activates more experts on harder tasks (*i.e.*, 2.23 *vs.* 2.84 for intra-benchmark and 2.58 *vs.* 3.43 for inter-benchmark).

Furthermore, we discover that the model with `Ada-K` excels at handling challenging tasks. Specifically, for the intra-benchmark dimension, our method demonstrates a moderate performance loss compared to the baseline with `Top-K` routing in ARC-E. However, when the task difficulty is increased to ARC-C, the model with `Ada-K` exhibits a performance advantage. Similar conclusions are even more evident in the inter-benchmark dimension. This indicates that, when faced with highly complex tasks, the flexibility of `Ada-K` in concentrating expert resources on key tokens enables more effective modeling of the tasks, leading to improved adaptability.

Equipped more layers with allocator yields better performance. In this section, we investigate the impact of varying allocator deployment ratios. By default, we integrate an allocator at each layer of the baseline models. The relevant results are presented in Table 9. All selected layers are sampled at equal intervals across the model. Our findings indicate that, due to the lightweight nature of the allocators, even when all layers are equipped with them, the number of trainable parameters remains minimal, resulting in only a negligible increase in time overhead. Moreover, while this effect does not significantly impact accuracy in benchmark evaluations, equipping more layers with an allocator clearly reduces computational overhead. Consequently, deploying allocators on a per-layer basis emerges as the optimal choice, as it enables a more refined expert allocation strategy at each layer, facilitating the scheduling of expert computations throughout the model.

5 Conclusion and Future Work

In this paper, we present a novel `Ada-K` routing strategy for MoE-based LLMs, which dynamically adjusts the number of activated experts based on token importance. `Ada-K` routing enhances the balance between computational efficiency and model performance through a lightweight allocator

module optimized via PPO algorithm. Extensive evaluations demonstrate that Ada-K routing significantly reduces expert activation by 30%-40% while improving benchmark performance across various MoE-based LLMs. This reduction in expert activation directly translates to computational gains, achieving more than a 25 % reduction in FLOPs and a 20% speedup in inference time, showcasing practical efficiency gains for large-scale applications. Moreover, this method is highly efficient, requiring minimal additional training, and can be easily integrated into existing MoE-based LLMs with low training overhead. Our analysis also provides valuable insights into adaptive resource allocation in large MoE models.

Our Ada-K routing strategy has proven to be an efficient post-training method for MoE-based LLMs. We believe that further validating its effectiveness during the whole model training stage is a valuable and interesting next step. Future work will involve training new MoE-based LLMs from scratch using our method. We anticipate that this approach will result in even highly-efficient LLMs, yielding more significant improvements in both performance and computational efficiency.

REFERENCES

Yuntao Bai, Andy Jones, Kamal Ndousse, Amanda Askell, Anna Chen, Nova DasSarma, Dawn Drain, Stanislav Fort, Deep Ganguli, Tom Henighan, et al. Training a helpful and harmless assistant with reinforcement learning from human feedback. *arXiv preprint arXiv:2204.05862*, 2022.

Edward Beeching, Clémentine Fourrier, Nathan Habib, Sheon Han, Nathan Lambert, Nazneen Rajani, Omar Sanseviero, Lewis Tunstall, and Thomas Wolf. Open llm leaderboard. https://huggingface.co/spaces/HuggingFaceH4/open_llm_leaderboard, 2023.

Steven Bird. Nltk: the natural language toolkit. In *Proceedings of the COLING/ACL 2006 Interactive Presentation Sessions*, pp. 69–72, 2006.

Sid Black, Stella Biderman, Eric Hallahan, Quentin Anthony, Leo Gao, Laurence Golding, Horace He, Connor Leahy, Kyle McDonell, Jason Phang, et al. Gpt-neox-20b: An open-source autoregressive language model. *arXiv preprint arXiv:2204.06745*, 2022.

Tom Brown, Benjamin Mann, Nick Ryder, Melanie Subbiah, Jared D Kaplan, Prafulla Dhariwal, Arvind Neelakantan, Pranav Shyam, Girish Sastry, Amanda Askell, et al. Language models are few-shot learners. *Advances in neural information processing systems*, 33:1877–1901, 2020a.

Tom Brown, Benjamin Mann, Nick Ryder, Melanie Subbiah, Jared D Kaplan, Prafulla Dhariwal, Arvind Neelakantan, Pranav Shyam, Girish Sastry, Amanda Askell, et al. Language models are few-shot learners. *Advances in neural information processing systems*, 33:1877–1901, 2020b.

Jie Cheng, Gang Xiong, Xingyuan Dai, Qinghai Miao, Yisheng Lv, and Fei-Yue Wang. Rime: Robust preference-based reinforcement learning with noisy preferences. *arXiv preprint arXiv:2402.17257*, 2024.

Wei-Lin Chiang, Zhuohan Li, Zi Lin, Ying Sheng, Zhanghao Wu, Hao Zhang, Lianmin Zheng, Siyuan Zhuang, Yonghao Zhuang, Joseph E Gonzalez, et al. Vicuna: An open-source chatbot impressing gpt-4 with 90%* chatgpt quality. *See https://vicuna. lmsys. org (accessed 14 April 2023)*, 2023.

Aidan Clark, Diego de Las Casas, Aurelia Guy, Arthur Mensch, Michela Paganini, Jordan Hoffmann, Bogdan Damoc, Blake Hechtman, Trevor Cai, Sebastian Borgeaud, et al. Unified scaling laws for routed language models. In *International conference on machine learning*, pp. 4057–4086. PMLR, 2022.

Peter Clark, Isaac Cowhey, Oren Etzioni, Tushar Khot, Ashish Sabharwal, Carissa Schoenick, and Oyvind Tafjord. Think you have solved question answering? try arc, the ai2 reasoning challenge. *arXiv preprint arXiv:1803.05457*, 2018.

Karl Cobbe, Vineet Kosaraju, Mohammad Bavarian, Mark Chen, Heewoo Jun, Lukasz Kaiser, Matthias Plappert, Jerry Tworek, Jacob Hilton, Reiichiro Nakano, et al. Training verifiers to solve math word problems. *arXiv preprint arXiv:2110.14168*, 2021.

Damai Dai, Chengqi Deng, Chenggang Zhao, RX Xu, Huazuo Gao, Deli Chen, Jiashi Li, Wangding Zeng, Xingkai Yu, Y Wu, et al. Deepseekmoe: Towards ultimate expert specialization in mixture-of-experts language models. *arXiv preprint arXiv:2401.06066*, 2024.

Erik Daxberger, Floris Weers, Bowen Zhang, Tom Gunter, Ruoming Pang, Marcin Eichner, Michael Emmersberger, Yinfei Yang, Alexander Toshev, and Xianzhi Du. Mobile v-moes: Scaling down vision transformers via sparse mixture-of-experts. *arXiv preprint arXiv:2309.04354*, 2023.

Nan Du, Yanping Huang, Andrew M. Dai, Simon Tong, Dmitry Lepikhin, Yuanzhong Xu, Maxim Krikun, Yanqi Zhou, Adams Wei Yu, Orhan Firat, Barret Zoph, Liam Fedus, Maarten P. Bosma, Zongwei Zhou, Tao Wang, Yu Emma Wang, Kellie Webster, Marie Pellat, Kevin Robinson, Kathleen S. Meier-Hellstern, Toju Duke, Lucas Dixon, Kun Zhang, Quoc V. Le, Yonghui Wu, Zhifeng Chen, and Claire Cui. Glam: Efficient scaling of language models with mixture-of-experts. In Kamalika Chaudhuri, Stefanie Jegelka, Le Song, Csaba Szepesvári, Gang Niu, and Sivan Sabato (eds.), *International Conference on Machine Learning, ICML 2022, 17-23 July 2022, Baltimore, Maryland, USA*, volume 162 of *Proceedings of Machine Learning Research*, pp. 5547–5569. PMLR, 2022a. URL https://proceedings.mlr.press/v162/du22c.html.

Nan Du, Yanping Huang, Andrew M Dai, Simon Tong, Dmitry Lepikhin, Yuanzhong Xu, Maxim Krikun, Yanqi Zhou, Adams Wei Yu, Orhan Firat, et al. Glam: Efficient scaling of language models with mixture-of-experts. In *International Conference on Machine Learning*, pp. 5547–5569. PMLR, 2022b.

David Eigen, Marc'Aurelio Ranzato, and Ilya Sutskever. Learning factored representations in a deep mixture of experts. *arXiv preprint arXiv:1312.4314*, 2013.

William Fedus, Barret Zoph, and Noam Shazeer. Switch transformers: Scaling to trillion parameter models with simple and efficient sparsity. *J. Mach. Learn. Res.*, 23:120:1–120:39, 2022a. URL http://jmlr.org/papers/v23/21-0998.html.

William Fedus, Barret Zoph, and Noam Shazeer. Switch transformers: Scaling to trillion parameter models with simple and efficient sparsity. *Journal of Machine Learning Research*, 23(120):1–39, 2022b.

Leo Gao, Jonathan Tow, Stella Biderman, Sid Black, Anthony DiPofi, Charles Foster, Laurence Golding, Jeffrey Hsu, Kyle McDonell, Niklas Muennighoff, Jason Phang, Laria Reynolds, Eric Tang, Anish Thite, Ben Wang, Kevin Wang, and Andy Zou. A framework for few-shot language model evaluation, September 2021. URL https://doi.org/10.5281/zenodo.5371628.

Kelvin Guu, Kenton Lee, Zora Tung, Panupong Pasupat, and Mingwei Chang. Retrieval augmented language model pre-training. In *International conference on machine learning*, pp. 3929–3938. PMLR, 2020.

Hussein Hazimeh, Zhe Zhao, Aakanksha Chowdhery, Maheswaran Sathiamoorthy, Yihua Chen, Rahul Mazumder, Lichan Hong, and Ed Chi. Dselect-k: Differentiable selection in the mixture of experts with applications to multi-task learning. *Advances in Neural Information Processing Systems*, 34:29335–29347, 2021.

Dan Hendrycks, Collin Burns, Steven Basart, Andy Zou, Mantas Mazeika, Dawn Song, and Jacob Steinhardt. Measuring massive multitask language understanding. *arXiv preprint arXiv:2009.03300*, 2020.

Ari Holtzman, Jan Buys, Li Du, Maxwell Forbes, and Yejin Choi. The curious case of neural text degeneration. *arXiv preprint arXiv:1904.09751*, 2019.

Quzhe Huang, Zhenwei An, Nan Zhuang, Mingxu Tao, Chen Zhang, Yang Jin, Kun Xu, Liwei Chen, Songfang Huang, and Yansong Feng. Harder tasks need more experts: Dynamic routing in moe models. *arXiv preprint arXiv:2403.07652*, 2024.

Robert A Jacobs, Michael I Jordan, Steven J Nowlan, and Geoffrey E Hinton. Adaptive mixtures of local experts. *Neural computation*, 3(1):79–87, 1991.

Albert Q Jiang, Alexandre Sablayrolles, Antoine Roux, Arthur Mensch, Blanche Savary, Chris Bamford, Devendra Singh Chaplot, Diego de las Casas, Emma Bou Hanna, Florian Bressand, et al. Mixtral of experts. *arXiv preprint arXiv:2401.04088*, 2024.

Jared Kaplan, Sam McCandlish, Tom Henighan, Tom B Brown, Benjamin Chess, Rewon Child, Scott Gray, Alec Radford, Jeffrey Wu, and Dario Amodei. Scaling laws for neural language models. *arXiv preprint arXiv:2001.08361*, 2020.

Teven Le Scao, Angela Fan, Christopher Akiki, Ellie Pavlick, Suzana Ilić, Daniel Hesslow, Roman Castagné, Alexandra Sasha Luccioni, François Yvon, Matthias Gallé, et al. Bloom: A 176b-parameter open-access multilingual language model. 2023.

Kimin Lee, Hao Liu, Moonkyung Ryu, Olivia Watkins, Yuqing Du, Craig Boutilier, Pieter Abbeel, Mohammad Ghavamzadeh, and Shixiang Shane Gu. Aligning text-to-image models using human feedback. *arXiv preprint arXiv:2302.12192*, 2023.

Dmitry Lepikhin, HyoukJoong Lee, Yuanzhong Xu, Dehao Chen, Orhan Firat, Yanping Huang, Maxim Krikun, Noam Shazeer, and Zhifeng Chen. Gshard: Scaling giant models with conditional computation and automatic sharding. *arXiv preprint arXiv:2006.16668*, 2020.

Mike Lewis, Shruti Bhosale, Tim Dettmers, Naman Goyal, and Luke Zettlemoyer. BASE layers: Simplifying training of large, sparse models. In Marina Meila and Tong Zhang (eds.), *Proceedings of the 38th International Conference on Machine Learning, ICML 2021, 18-24 July 2021, Virtual Event*, volume 139 of *Proceedings of Machine Learning Research*, pp. 6265–6274. PMLR, 2021a. URL http://proceedings.mlr.press/v139/lewis21a.html.

Mike Lewis, Shruti Bhosale, Tim Dettmers, Naman Goyal, and Luke Zettlemoyer. Base layers: Simplifying training of large, sparse models. In *International Conference on Machine Learning*, pp. 6265–6274. PMLR, 2021b.

Raymond Li, Loubna Ben Allal, Yangtian Zi, Niklas Muennighoff, Denis Kocetkov, Chenghao Mou, Marc Marone, Christopher Akiki, Jia Li, Jenny Chim, et al. Starcoder: may the source be with you! *arXiv preprint arXiv:2305.06161*, 2023.

Stephanie Lin, Jacob Hilton, and Owain Evans. Truthfulqa: Measuring how models mimic human falsehoods. *arXiv preprint arXiv:2109.07958*, 2021.

Ilya Loshchilov and Frank Hutter. Decoupled weight decay regularization. *arXiv preprint arXiv:1711.05101*, 2017.

Reiichiro Nakano, Jacob Hilton, Suchir Balaji, Jeff Wu, Long Ouyang, Christina Kim, Christopher Hesse, Shantanu Jain, Vineet Kosaraju, William Saunders, et al. Webgpt: Browser-assisted question-answering with human feedback. *arXiv preprint arXiv:2112.09332*, 2021.

Long Ouyang, Jeffrey Wu, Xu Jiang, Diogo Almeida, Carroll Wainwright, Pamela Mishkin, Chong Zhang, Sandhini Agarwal, Katarina Slama, Alex Ray, et al. Training language models to follow instructions with human feedback. *Advances in Neural Information Processing Systems*, 35: 27730–27744, 2022.

Mikołaj Piórczyński, Filip Szatkowski, Klaudia Bałazy, and Bartosz Wójcik. Exploiting transformer activation sparsity with dynamic inference. *arXiv preprint arXiv:2310.04361*, 2023.

Colin Raffel, Noam Shazeer, Adam Roberts, Katherine Lee, Sharan Narang, Michael Matena, Yanqi Zhou, Wei Li, and Peter J Liu. Exploring the limits of transfer learning with a unified text-to-text transformer. *The Journal of Machine Learning Research*, 21(1):5485–5551, 2020.

Carlos Riquelme, Joan Puigcerver, Basil Mustafa, Maxim Neumann, Rodolphe Jenatton, André Susano Pinto, Daniel Keysers, and Neil Houlsby. Scaling vision with sparse mixture of experts. *Advances in Neural Information Processing Systems*, 34:8583–8595, 2021.

Anna Rogers, Olga Kovaleva, and Anna Rumshisky. A primer in bertology: What we know about how bert works. *Transactions of the Association for Computational Linguistics*, 8:842–866, 2021.

Stephen Roller, Sainbayar Sukhbaatar, Jason Weston, et al. Hash layers for large sparse models. *Advances in Neural Information Processing Systems*, 34:17555–17566, 2021.

Keisuke Sakaguchi, Ronan Le Bras, Chandra Bhagavatula, and Yejin Choi. Winogrande: An adversarial winograd schema challenge at scale. *Communications of the ACM*, 64(9):99–106, 2021.

Timo Schick and Hinrich Schütze. Exploiting cloze questions for few shot text classification and natural language inference. *arXiv preprint arXiv:2001.07676*, 2020.

Noam Shazeer, Azalia Mirhoseini, Krzysztof Maziarz, Andy Davis, Quoc Le, Geoffrey Hinton, and Jeff Dean. Outrageously large neural networks: The sparsely-gated mixture-of-experts layer. *arXiv preprint arXiv:1701.06538*, 2017a.

Noam Shazeer, Azalia Mirhoseini, Krzysztof Maziarz, Andy Davis, Quoc V. Le, Geoffrey E. Hinton, and Jeff Dean. Outrageously large neural networks: The sparsely-gated mixture-of-experts layer. In *5th International Conference on Learning Representations, ICLR 2017, Toulon, France, April 24-26, 2017, Conference Track Proceedings*. OpenReview.net, 2017b. URL https://openreview.net/forum?id=B1ckMDqlg.

Nisan Stiennon, Long Ouyang, Jeffrey Wu, Daniel Ziegler, Ryan Lowe, Chelsea Voss, Alec Radford, Dario Amodei, and Paul F Christiano. Learning to summarize with human feedback. *Advances in Neural Information Processing Systems*, 33:3008–3021, 2020.

Richard S Sutton and Andrew G Barto. *Reinforcement learning: An introduction*. MIT press, 2018.

Mirac Suzgun, Nathan Scales, Nathanael Schärli, Sebastian Gehrmann, Yi Tay, Hyung Won Chung, Aakanksha Chowdhery, Quoc V Le, Ed H Chi, Denny Zhou, et al. Challenging big-bench tasks and whether chain-of-thought can solve them. *arXiv preprint arXiv:2210.09261*, 2022.

Rohan Taori, Ishaan Gulrajani, Tianyi Zhang, Yann Dubois, Xuechen Li, Carlos Guestrin, Percy Liang, and Tatsunori B Hashimoto. Alpaca: A strong, replicable instruction-following model. *Stanford Center for Research on Foundation Models. https://crfm. stanford. edu/2023/03/13/alpaca. html*, 3(6):7, 2023.

Qwen Team. Qwen1.5-moe: Matching 7b model performance with 1/3 activated parameters. https://qwenlm.github.io/blog/qwen-moe/. Accessed: 2024-03-28.

Hugo Touvron, Thibaut Lavril, Gautier Izacard, Xavier Martinet, Marie-Anne Lachaux, Timothée Lacroix, Baptiste Rozière, Naman Goyal, Eric Hambro, Faisal Azhar, et al. Llama: Open and efficient foundation language models. *arXiv preprint arXiv:2302.13971*, 2023a.

Hugo Touvron, Louis Martin, Kevin Stone, Peter Albert, Amjad Almahairi, Yasmine Babaei, Nikolay Bashlykov, Soumya Batra, Prajjwal Bhargava, Shruti Bhosale, et al. Llama 2: Open foundation and fine-tuned chat models. *arXiv preprint arXiv:2307.09288*, 2023b.

Ashish Vaswani, Noam Shazeer, Niki Parmar, Jakob Uszkoreit, Llion Jones, Aidan N Gomez, Łukasz Kaiser, and Illia Polosukhin. Attention is all you need. *Advances in neural information processing systems*, 30, 2017.

Jiazheng Xu, Xiao Liu, Yuchen Wu, Yuxuan Tong, Qinkai Li, Ming Ding, Jie Tang, and Yuxiao Dong. Imagereward: Learning and evaluating human preferences for text-to-image generation. *arXiv preprint arXiv:2304.05977*, 2023.

Tongtian Yue, Jie Cheng, Longteng Guo, Xingyuan Dai, Zijia Zhao, Xingjian He, Gang Xiong, Yisheng Lv, and Jing Liu. Sc-tune: Unleashing self-consistent referential comprehension in large vision language models. *arXiv preprint arXiv:2403.13263*, 2024.

Rowan Zellers, Ari Holtzman, Yonatan Bisk, Ali Farhadi, and Yejin Choi. Hellaswag: Can a machine really finish your sentence?, 2019.

Yanqi Zhou, Tao Lei, Hanxiao Liu, Nan Du, Yanping Huang, Vincent Zhao, Andrew M Dai, Quoc V Le, James Laudon, et al. Mixture-of-experts with expert choice routing. *Advances in Neural Information Processing Systems*, 35:7103–7114, 2022.

Barret Zoph, Irwan Bello, Sameer Kumar, Nan Du, Yanping Huang, Jeff Dean, Noam Shazeer, and William Fedus. St-moe: Designing stable and transferable sparse expert models. *arXiv preprint arXiv:2202.08906*, 2022.

Simiao Zuo, Xiaodong Liu, Jian Jiao, Young Jin Kim, Hany Hassan, Ruofei Zhang, Tuo Zhao, and Jianfeng Gao. Taming sparsely activated transformer with stochastic experts. *arXiv preprint arXiv:2110.04260*, 2021.

A Evaluation Benchmarks

Following previous works (Team; Jiang et al., 2024; Dai et al., 2024), we assess models across six standard benchmarks utilizing the Eleuther AI Language Model Evaluation Harness, a comprehensive framework designed to evaluate generative language models on a diverse array of tasks. In these evaluations, higher scores indicate better performance. We selected these benchmarks because they assess a range of reasoning abilities and general knowledge across multiple disciplines in both zero-shot and few-shot scenarios.

Table 10: Details of benchmarks. We follow the setting of HuggingFace Open LLM Leaderboard.

Benchmark	#shots	# Samples	Details
ARC-C (Clark et al., 2018)	25	2.59k	A set of grade-school science questions.
HellaS (Zellers et al., 2019)	10	70k	A test of commonsense inference, which is easy for humans but challenging for SOTA models.
MMLU (Hendrycks et al., 2020)	5	14.9k	A test to measure a text model's multitask accuracy. The test covers 57 tasks including elementary mathematics, US history, computer science, law, and more.
GSM8K (Cobbe et al., 2021)	5	8.5k	Diverse grade school math word problems to measure a model's ability to solve multi-step mathematical reasoning problems.
TruthQA (Lin et al., 2021)	0	0.8k	A test to measure a model's propensity to reproduce falsehoods commonly found online.
WinoG (Sakaguchi et al., 2021)	5	44k	An adversarial and difficult Winograd benchmark at scale, for commonsense reasoning.

B Implementation Details

In this section, we detail the training protocols of the proposed framework. The specific hyper-parameter configurations for training are reported in Table 11. These protocols are applicable to all the baseline models, utilizing 8 A800-80G GPUs. Throughout all training phases, we consistently conduct a single epoch to prevent overfitting. The batch size per GPU is set at 8. Gradient checkpointing is activated for both training phases to enhance memory efficiency.

Table 11: Additional training details.

Configuration	Fine-tuning	
	Warm-Start	PPO
Optimizer	AdamW	AdamW
Base LR	1e-3	1e-3
Precision	bf16	bf16
Weight Decay	0.1	0.1
Batch Size	64	64
LR Decay Schedule	cosine	constant
Gradient Checkpoint	True	True
Training Epochs	1	1
Max Length	2048	2048
Threshold p	0.3	–
Regularization Coef	–	3e-3
PPO Epoch	–	2

C Training Data

In this section, we introduce the data utilized in our training. For default setting, we employ a dataset comprising 10k randomly sampled from mainstream public supervised fine-tuning datasets. Additionally, the sources of the pretrain corpora used in the ablation experiments are also reported in Table 12. All these data are widely employed in the training of prevalent LLMs (Touvron et al., 2023a; Taori et al., 2023; Chiang et al., 2023).

Table 12: Datasets used for training. We collect data from various sources to empower the model with a broad spectrum of linguistic capabilities. We ensure that all datasets are publicly available in the community.

Usage	**Source**	**#Sample**
Supervised Fine-tuning	Alpaca GPT4, UltraChat 200k, LIMA, OpenPlatypus CodeAlpaca 20k, Wiki QA, MathInstruct	10.2k
Pretrain	Wiki Demo, RedPajama V2, Wikipedia, StarCoder	10.1k